Acceleration of Magnetized Plasmoid by Pulsed Magnetic Coil*)

Taichi SEKI, Tomohiko ASAI, Daichi KOBAYASHI, Ryotaro YANAGI, Hiroshi GOTA[1)], Thomas ROCHE[1)] and Tadafumi MATSUMOTO[1,2)]

College of Science and Technology, Nihon University, Tokyo 101-8308, Japan
[1)]*TAE Technologies, Inc., Foothill Ranch, CA 92610, USA*
[2)]*University of California at Irvine, Irvine, CA 92697, USA*

(Received 16 November 2020 / Accepted 23 December 2020)

Compact toroid injection has been proposed as a particle fueling technique for the core region of fusion plasmas. An accelerated plasmoid penetrates through confinement magnetic fields and reaches the core region of target plasmas. To inject plasmoids into the magnetically confined plasmas featuring strong confinement fields, the injection velocity should be increased. The injection velocity depends on the operating conditions of the compact toroid injector such as charging voltage and gas pressure. Changing these conditions is not preferable as it affected not only the injection velocity but also other plasmoid parameters. Pulsed magnetic coil has been introduced for the additional acceleration of the ejected plasmoid. The pulsed field was produced by the current flowing through a one-turn coil installed at the muzzle of the magnetized coaxial plasma gun. The acceleration of ejected plasmoid by pulsed magnetic coil was experimentally verified. Application of pulsed magnetic field resulted in velocity increase up to approximately 50% compared to the average velocity without additional acceleration.

Keywords: magnetized coaxial plasma gun, compact toroid injection, compact toroid, magnetized plasmoid, fueling

DOI: 10.1585/pfr.16.2401020

1. Introduction

Compact Toroid (CT) injection has been proposed as one of the particles fueling methods for magnetically confined plasmas [1]. In this method, plasmoids are usually formed by a magnetized coaxial plasma gun (MCPG) and injected into the core region of fusion plasmas by penetrating through the confinement field. CT injection experiments have been conducted on tokamaks [2–4] and field-reversed pinches [5] for fueling and/or helicity injection.

CT injection experiment for particle fueling in large field-reversed configuration (FRC) plasmas was conducted at C-2/C-2U facility of TAE Technologies, Inc [6]. In this study, multi-pulsed CT injection fueling with 1 kHz of repetition frequency was made by two CT injectors. Plasmoids were injected into FRC plasma at velocities exceeding 100 km/s. Successful fueling was demonstrated without any serious deleterious effects on the target plasma and total particle inventory increased by 20 - 30% per single CT injection [6–8].

The injection velocity is one of the key parameters to determine the penetration depth. To inject plasmoids into magnetically confined plasma with a strong confinement field, injection velocity should be increased. A one-turn pulse coil is installed at the muzzle of the MCPG to control the injection velocity of the magnetized plasmoids from the CT injector. The pulse coil produce the pulsed magnetic field when the plasmoid pass through it. If the current in pulse coil was applied in the direction opposite to the toroidal current of the plasmoid and plasma was located directly under the pulse coil, the magnetic pressure formed by the pulsed field accelerated the plasmoid. Moreover, tearing reconnection behind the plasmoid is induced. It is expected that the trailing low-temperature plasma can be separated from the plasmoid. In addition, if the direction of the current flowing through the pulse coil and the toroidal current in the plasmoid coincided, the plasma climbed the "valley" of the pulsed field potential. In this case, the plasmoid was decelerated after passing under the pulse coil.

In this paper, we report the experimental results of additional plasmoid acceleration by the pulsed magnetic coil. In case of pulsed magnetic field applied, velocity of plasmoids from CT injector increased by up to 50% compared to the average velocity without pulsed field.

2. CT Injector (Magnetized Coaxial Plasma Gun)

CT injector developed in this study is a typical single staged MCPG and is shown in Fig. 1. It consists of coaxially arranged inner and outer electrodes, a center solenoidal bias coil with an iron core [9], and gas puff valves. This MCPG is similar CT injector installed at the C-2/C-2U facility. It has the outer diameter of the inner

author's e-mail: csta19012@g.nihon-u.ac.jp

*) This article is based on the presentation at the 29th International Toki Conference on Plasma and Fusion Research (ITC29).

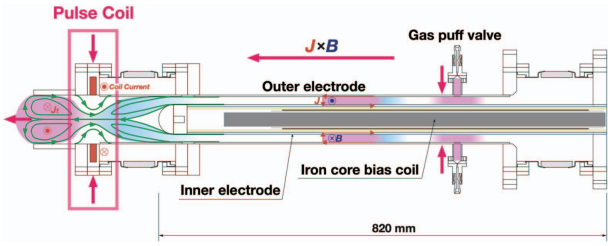

Fig. 1 Acceleration mechanism of CT by applied pulsed magnetic field.

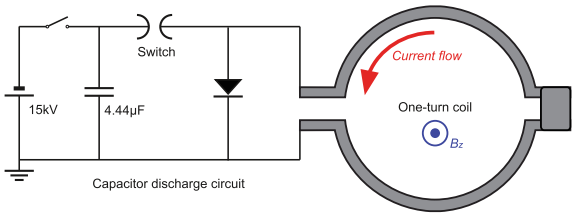

Fig. 2 Diagram of the pulsed magnetic coil with the discharge circuit.

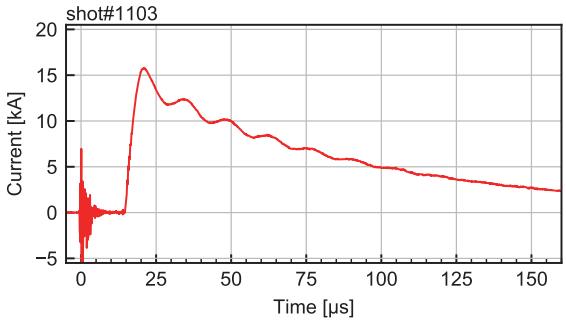

Fig. 3 The current waveform of the pulsed magnetic coil.

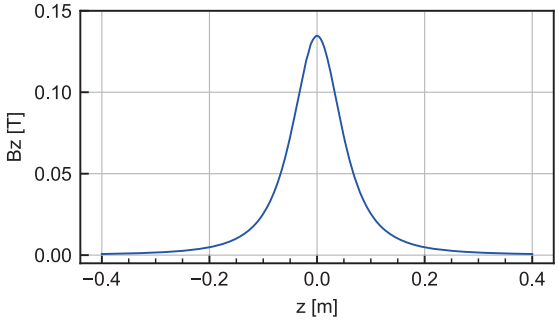

Fig. 4 The calculated profile of a pulsed magnetic field when the current is 15 kA.

electrode of 54.0 mm and the inner diameter of the outer electrode of 83.1 mm. The coaxial electrodes are connected to 9.6 μF capacitor banks charged at 20 kV. The peak value of the gun current is ~130 kA and its rise time is ~2 μs.

The typical formation process for a magnetized plasmoid generated by MCPG includes several stages as follows. First, the deuterium gas injected from valves is pre-ionized and injected between the inner and outer electrodes. Next, high voltage is applied to the gap between the electrodes. It results in plasma generation and its acceleration by J × B Lorenz self-force. Here $\boldsymbol{J}$ is the discharge current at MCPG and $\boldsymbol{B}$ is the magnetic field generated by the discharge current. An accelerated plasma captures the bias magnetic flux applied by the center solenoidal coil. Finally, the spheromak-like plasmoid that contains both toroidal and poloidal fluxes is ejected. The poloidal field strength of a plasmoid is 0.01 - 0.03 T and depends on the strength of the bias field. Pulsed magnetic field is about 10 times the poloidal field of the plasmoid. In this experiment, we verified the effect of additional acceleration via magnetic pressure by applying pulsed field to the plasmoids generated and ejected by MCPG.

3. Acceleration by Pulsed Magnetic Coil

One-turn pulse coil with a radius of 70 mm is installed at the muzzle of the MCPG to accelerate the ejected plasmoids. It is separately driven from the MCPG by the crowbar discharge circuit as shown in Fig. 2. The current through one-turn pulse coil circulates in a circuit with a diode connected in parallel as shown in Fig. 3. It produces localized pulsed magnetic field when the plasmoids pass through. Figure 4 shows the calculated profile of the pulsed magnetic field along the ejection axis (z-axis) when the current is set to 15 kA. In this case, pulsed magnetic field reaches 0.13 T at the pulse coil centerline ($z = 0$).

The direction of the pulsed field coincides with that of the poloidal field at the outer part of a plasmoid. At the same time, the direction of the current flowing through the pulse coil and the toroidal current in the plasmoid are opposite as shown in Fig. 1. The plasmoid obtains potential energy from pulsed field when it passes through the pulse coil. The difference in magnetic potential between front and back surfaces of the plasmoid contribute to plasmoid acceleration. Let us assume that plasmoid can be modeled as a rigid body with infinite conductivity. Then the balance between magnetic potential energy and kinetic energy of plasmoid reads as

$$\int \frac{\Delta B^2}{\mu_0} dV + \frac{1}{2} m v_0{}^2 = \frac{1}{2} m (v_0 + \Delta v)^2, \quad (1)$$

where $\boldsymbol{\Delta B}$ is the change in magnetic flux density between front and back surfaces of a plasmoid, $\boldsymbol{m}$ is the mass of a plasmoid, $\boldsymbol{v}_0$ is the plasmoid initial velocity, and $\boldsymbol{\Delta v}$ is the velocity increment. The integration is carried out over the region under the magnetic pressure. With $\boldsymbol{m} = 5 \times 10^{-9}$ kg and pulse field strength of 0.13 T, velocity increment can be determined from Eq. (1) and amounts to 33.2 km/s. This model does not consider plasmoid deformation as its entire magnetic potential energy transforms to a kinetic one.

4. Experimental Setup

The schematic of the experimental setup is shown in Fig. 5. It includes three components, namely MCPG, drift tube, and quartz vacuum vessel. The pulse coil was inserted between MCPG and drift tube. All plasmoid parameters were measured in the drift tube. The set of photomultiplier tubes (PMT1 and 2) with collimated fibers served to observe radiation from ejected plasmoids. Plasmoid velocities were estimated by the time-of-flight method that compared the time of the rising edges of the radiation intensity at z = 100 and 380 mm. The triple probe was mounted at z = 380 mm to estimate electron density and temperature.

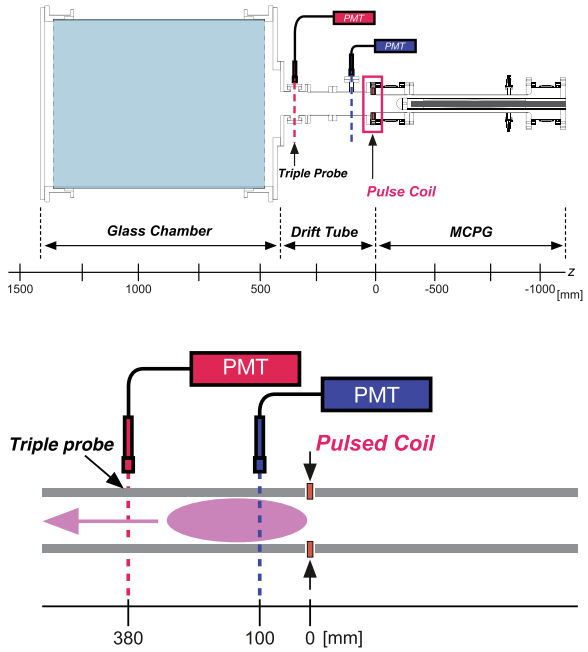

Fig. 5 Experimental setup and diagnostics.

5. Experimental Results and Discussion

Figure 6 shows the radiation intensity of the plasmoids in the drift tube. Here, t = 0 is the breakdown time of CT injector. Plasmoid velocity in absence of pulsed field is shown in Fig. 6 (a) and amounts to 34.6 km/s. When the pulsed field was introduced, it increased to 37.8 km/s (Fig. 6 (b)). The difference between two cases was 3.2 km/s that was small compared to the velocity increment of 33.2 km/s estimated from Eq. (1). The radiation signal at z = 100 mm was ringing with the current at the pulse coil. Supposedly, plasmoid was affected by the oscillation of the pulsed field. The oscillation component was damped at z = 380 mm. Figure 7 shows electron temperature and density at z = 380 mm. There was no significant difference in electron temperatures, but the electron density increased dramatically when the pulsed field was applied (arrow in Fig. 7 (b)).

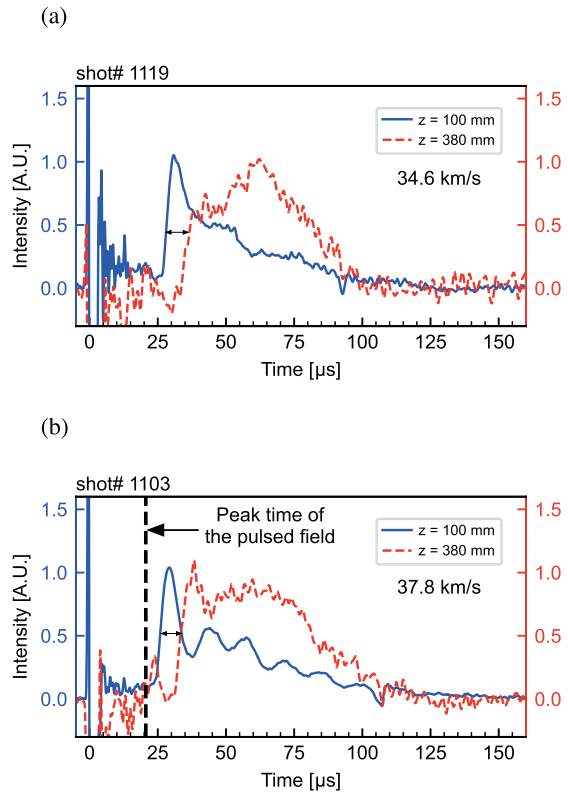

Fig. 6 Radiation intensity at z = 100 and 380 mm, (a) without the pulsed magnetic field and (b) with the pulsed magnetic field.

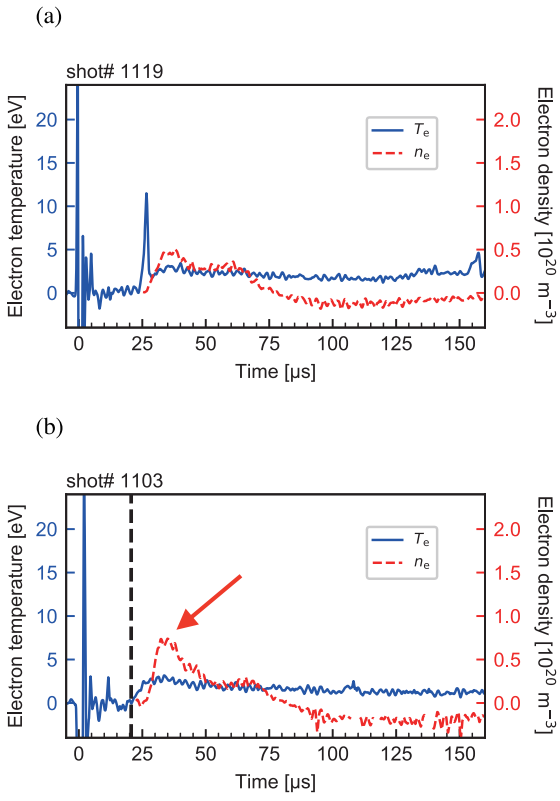

Fig. 7 Electron temperature and density at z = 380 mm, (a) without the pulsed magnetic field and (b) with the pulsed magnetic field.

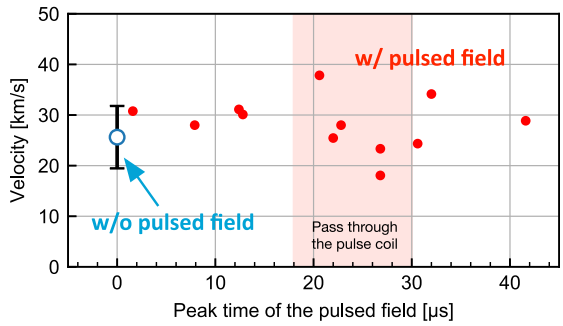

Fig. 8 Comparison of ejection velocity withand without the pulsed magnetic field.

Ejection velocities for both cases were plotted in Fig. 8 with horizontal axis corresponding to the peak times of the pulsed field. The colored area (18 - 30 μs) represented time interval when ejected plasmoids passed under the pulse coil. The open blue circle at $t = 0$ corresponded to the plasmoid velocity (25.6 km/s) averaged for 15 shots in absence of pulsed field with error bar indicating the standard deviation. The red dots show a single shot for each value of the pulsed field. Plasmoid velocities obtained in presence of pulsed field exceeded average velocity in its absence. In particular, for the peak time of 20.6 μs, the velocity increases by about 50% compared to the average velocity without the pulsed field applied. It was equivalent to 36.7% of the velocity increment estimated from Eq. (1). This discrepancy can be attributed to the fact that Eq. (1) corresponds to the model with ideal acceleration conditions. In reality, plasmoid deformation and pulsed-field application time should be also considered. The effect of additional acceleration by the pulsed field depends on the field application time.

6. Summary

One-turn pulse coil at the muzzle of CT injector allowed for additional acceleration of ejected plasmoids. Application of pulsed magnetic field resulted in 50% increase in plasmoid velocity compared to the case without additional acceleration. The increment of ejection velocity depended on the time point for which pulsed magnetic field was applied. Further optimization is required to obtain the best performance of additional acceleration by pulsed magnetic field.

Acknowledgment

The authors would like to acknowledge all members of Fusion-Plasma group, Nihon University and TAE Technologies. This work was partially supported by JSPS KAKENHI Grant Number JP20H0043, JP19K21868 and Nihon University, College of Science and Technology, Grants-in-Aid, Grant for Project Research.

[1] L.J. Perkins *et al.*, Nucl. Fusion **28**, 1365 (1988).
[2] R. Raman *et al.*, Nucl. Fusion **37**, 967 (1997).
[3] C. Xiao *et al.*, Phys. Plasmas **11**, 4041 (2004).
[4] M. Nagata *et al.*, Nucl. Fusion **45**, 1056 (2005).
[5] T. Asai *et al.*, J. Plasma Fusion Res. **81**, 335 (2005).
[6] T. Matsumoto *et al.*, Rev. Sci. Instrum. **87**, 053512 (2016).
[7] H. Gota *et al.*, Nucl. Fusion **57**, 116021 (2017).
[8] T. Asai *et al.*, Nucl. Fusion **57**, 076018 (2017).
[9] T. Edo *et al.*, J. Plasma Fusion. Res. **13**, 3405062 (2018).